Preparation of coherent superposition in a three-state system by adiabatic passage

N. Sangouard,[1,2,*] S. Guérin,[2,†] L. P. Yatsenko,[1,‡] and T. Halfmann[1,§]
[1]*Fachbereich Physik, Universität Kaiserslautern, 67653 Kaiserslautern, Germany*
[2]*Laboratoire de Physique de l'Université de Bourgogne, UMR CNRS 5027, BP 47870, 21078 Dijon, France*
(Received 30 March 2004; published 29 July 2004)

We examine the topology of eigenenergy surfaces associated to a three-state system driven by two quasi-resonant fields. We deduce mechanisms that allow us to generate various coherent superposition of two states using an additional field, far off resonances. We report the numerical validations in mercury atoms as a model system, creating the coherent superpositions of two excited states and of two states coupled by a Raman process.

DOI: 10.1103/PhysRevA.70.013415 PACS number(s): 42.50.Hz, 32.80.−t

I. INTRODUCTION

The preparation of atoms and molecules in coherent superpositions of states has attracted the attention of physicists since it gives rise to interesting applications. In nonlinear optics, an initial atomic coherence improves considerably the efficiency of the traditional nonlinear frequency conversion processes in gases [1–11] and novel laser sources can be created. Other fields of application are in relation with the control of chemical reactions [12] and quantum information [13,14].

Coherent superpositions of states can be generated, in a robust way with respect to the variation of the field parameters, using processes based on adiabatic passage. It has been suggested [15–19] and experimentally demonstrated [20] that the technique of half stimulated Raman adiabatic passage (half-STIRAP) can be used to prepare such coherent superpositions. In this technique two delayed, but partially overlapping pulses—pump and Stokes—with the Stokes-laser following the pump laser pulse, induce a coherent superposition of two states in a Raman-type linkage. This coherent superposition emerges from a unique dark state which does not give any relative dynamical phase between the two components of the superposition, apart from the optical phase $(\omega_s-\omega_p)t$ (where ω_s and ω_p are the Stokes and pump frequency). However, it is necessary that the pulses vanish together, of a ratio maintained constant, which may be difficult in practice to realize.

An extension of STIRAP, called tripod-STIRAP [21,22], allows the creation of a coherent superposition of two states in a four-state system by the interaction with three pulses. The weights of each component of the superposition are controlled by the ordering of pulses, the delays between them and their intensities. The mechanism is based on a non-Abelian geometric phase coming from two instantaneous degenerate dark states.

The technique of half Stark-chirped rapid adiabatic passage (half-SCRAP) is a simple and robust process to prepare a coherent superposition of two states [23,24]. In half-SCRAP two laser pulses, a resonant pump pulse and a far off-resonant Stark pulse, are introduced into the system. The relative phase between the two states of the coherent superposition is controlled by the order of the pulse sequence: for the Stark laser preceding the pump pulse, the population dynamics are governed by a single eigenstate, leading to an optical phase $\omega_p t$ (ω_p being the frequency of the pump). For the Stark laser following the pump pulse, the pump laser lifts the degeneracy by creating two eigenstates that govern the dynamics. This induces an additional relative dynamical phase.

In this paper, we extend the principle of half-SCRAP to a three-state system driven by two quasi-resonant fields and a far off-resonant Stark field. The Stark laser introduces level crossings, offering some additional connections between the states.

The analysis is based on Refs. [24–26]: from an effective Hamiltonian in the usual rotating wave approximation combined with an adiabatic elimination of the nonresonant states, we calculate the surfaces of the three-state system as a function of two field amplitudes. The topology of these energy surfaces exhibits conical intersections and avoided crossings. We design a path on these surfaces, i.e., we choose the amplitudes of the pulses as well as the delay in order to connect the initial state to a target coherent superposition of states. Using an additional Stark laser, we are able to modify the topology of the energy surfaces (the creation or suppression of a conical intersection) in order to design other coherent superpositions that are not topologically accessible otherwise. For a given initially populated state, we thus show that any superposition of two of the three states can be generated. In Sec. II we present the topology of the eigenenergy surfaces associated to the three-state Hamiltonian with two quasi-resonant fields and the paths on these surfaces from the ground state to the superposition of two states in Λ-, ladder-, or V-type configurations. In all cases, the relative phase of the components of the superposition does not depend on the pulse area if a particular sequence is chosen. Furthermore, their weights are adjustable by varying the frequency of one of the two fields. These processes involve a combination of avoided crossing (adiabatic) and exact crossing (diabatic) dy-

*Email address: nicolas.sangouard@u-bourgogne.fr
†Email address: sguerin@u-bourgogne.fr
‡Permanent address: Institute of Physics, Ukrainian Academy of Sciences, prospect Nauki 46, Kiev-22, 252650 Ukraine.
§Email address: halfmann@physik.uni-kl.de

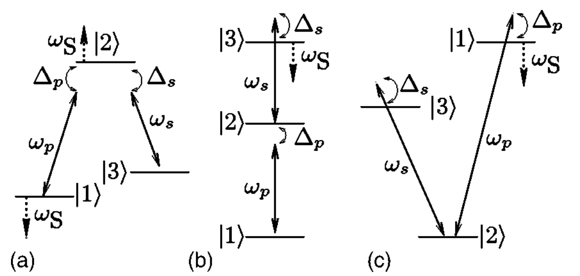

FIG. 1. Schematic energy-level diagram in (a) Λ, (b) ladder, and (c) V configuration. The direction of the dashed arrows represents the direction of the Stark shift. All the population of the system is set in the ground state at the beginning of the interaction.

namics. The conditions for an optimized realization of these adiabatic and diabatic passages are analyzed in Sec. III. We propose a systematic method to find the pulse parameters that minimize both nonadiabatic and nondiabatic losses associated to the adiabatic and diabatic dynamics. In Sec. IV, we show that the coherent superposition of two states coupled by a Raman process can be prepared using an additional Stark laser. We discuss mechanisms adapted to Λ-, ladder- and V-type configurations. Finally, we propose an experimental implementation in mercury atoms.

II. THE TOPOLOGY FOR STIMULATED ADIABATIC PASSAGE

In this section, we analyze the topology of the eigenvalues of the effective Hamiltonian as a function of the Rabi frequency parameters as developed in [25–27] for the particular problem of the creation of coherent superposition of states. Additional features involve quasidegeneracies that appear at the beginning or at the end of the process and that have to be treated specifically [28].

The essence of a stimulated adiabatic passage by delayed pulses is captured in the Hamiltonian obtained by rotating wave approximation (RWA),

$$H(t)=\frac{\hbar}{2}\begin{pmatrix}0 & \Omega_p(t) & 0\\ \Omega_p(t) & 2\Delta_p & \Omega_s(t)\\ 0 & \Omega_s(t) & 2(\Delta_p-\Delta_s)\end{pmatrix}. \tag{1}$$

As shown in Fig. 1, it describes the interaction between the three-state system (states $|1\rangle$, $|2\rangle$ and $|3\rangle$) and the two quasi-resonant laser fields: the pump and Stokes laser, which excite the $|1\rangle$-$|2\rangle$ and $|2\rangle$-$|3\rangle$ transition with Rabi frequencies $\Omega_p=\mu_{12}\mathcal{E}_p/\hbar$ and $\Omega_s=\mu_{23}\mathcal{E}_s/\hbar$, μ_{12} and μ_{23} being the transition moments of the $|1\rangle$-$|2\rangle$ and $|2\rangle$-$|3\rangle$ pairs and $\mathcal{E}_j$, $j=p,s$, the amplitude of the j field. ϕ_j, $j=p,s$ is the initial phase of the classical fields that generate a global field of amplitude,

$$\mathcal{E}(t)=\mathcal{E}_p\cos(\omega_p t+\phi_p)+\mathcal{E}_s\cos(\omega_s t+\phi_s). \tag{2}$$

The frequencies ω_p, ω_s are detuned from the Bohr frequencies of the $|1\rangle$-$|2\rangle$ and the $|2\rangle$-$|3\rangle$ pairs by Δ_p and Δ_s. For Λ-, ladder-, and V-type systems, these two one-photon detunings are defined as

$$(\Lambda)\quad \hbar\Delta_p=E_2-E_1-\hbar\omega_p,\quad \hbar\Delta_s=E_2-E_3-\hbar\omega_s, \tag{3a}$$

$$(\text{ladder})\quad \hbar\Delta_p=E_2-E_1-\hbar\omega_p,\quad \hbar\Delta_s=E_2-E_3+\hbar\omega_s, \tag{3b}$$

$$(\text{V})\quad \hbar\Delta_p=E_2-E_1+\hbar\omega_p,\quad \hbar\Delta_s=E_2-E_3+\hbar\omega_s, \tag{3c}$$

where E_1, E_2 and E_3 are the energies of the states $|1\rangle$, $|2\rangle$ and $|3\rangle$. The validity of the RWA for time varying amplitudes requires the following two conditions: (i) limiting field amplitudes $\Omega_k^{\max}\ll\omega_k$ where $k=\{s,p\}$ and (ii) limiting pulse durations $\Delta^{\mathrm{NR}}T\gg 1$ where the nonresonant detuning $\Delta^{\mathrm{NR}}=\min(E_i-E_j\pm\omega_k)\neq\{\Delta_p,\Delta_s\}$ with $\{i,j\}=\{1,2\}$ and T characterizes the pulse shape durations [which is, e.g., the full width half maximum (FWHM) for a Gaussian pulse]. The Hamiltonian (1) is written in the basis

$$(\Lambda)\quad \{|1\rangle,|2\rangle e^{-i\phi_p},|3\rangle e^{-i(\phi_p-\phi_s)}\}, \tag{4a}$$

$$(\text{ladder})\quad \{|1\rangle,|2\rangle e^{-i\phi_p},|3\rangle e^{-i(\phi_p+\phi_s)}\}, \tag{4b}$$

$$(\text{V})\quad \{|1\rangle,|2\rangle e^{i\phi_p},|3\rangle e^{i(\phi_p-\phi_s)}\}, \tag{4c}$$

in the cases (a), (b) and (c) of Fig. 1. We have assumed that the $|1\rangle$-$|3\rangle$ pair has no (or negligible) coupling and that the spontaneous emission is negligibly small on the time scale of the pulse durations.

We will examine the topology of the eigenenergy surfaces for various sequences of the pump and Stokes laser (see an example in Fig. 2 described later). The topology depends on the detunings that determine the relative position of the energy at the origin. We first analyze how to construct a coherent superposition of the states, with equal weights, i.e. of the type

$$\frac{1}{\sqrt{2}}(|i\rangle+e^{i\phi}|j\rangle). \tag{5}$$

This requires one of the two detunings (3) to be zero. Increasing the amplitude of the associated resonant laser lifts the degeneracy and the populations are equally split in two paths. By a judicious choice of (Ω_p,Ω_s), we design paths from the initial state to a preselected coherent superposition of states. We determine the delay between the two pulses, as well as their durations and their intensities required to follow the chosen path and to generate the target coherent state.

Considering positive Rabi frequencies and denoting the two photon detuning,

$$\delta=\Delta_p-\Delta_s, \tag{6}$$

we have two generic cases for $\delta>0$ and two symmetric (and thus equivalent) cases for $\delta<0$.

We consider here $\delta>0$ without loss of generality. The two generic cases are labeled 12-3 and 1-32 in which $\Delta_p=0$ and $\Delta_s=0$, respectively.

The case 12-3, i.e. $\Delta_s/\delta=-1$, is depicted in Fig. 2. In the plane $\Omega_s=0$, the three eigenvalues of the effective Hamiltonian (1)

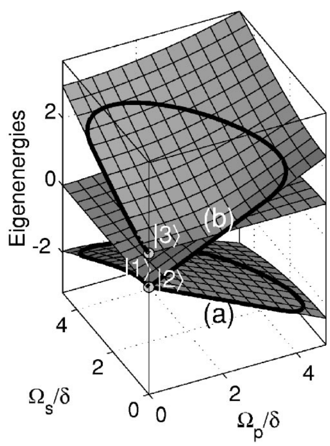

FIG. 2. Surfaces of eigenenergies as functions of the two Rabi frequencies Ω_p and Ω_s (in δ units) for the 12-3 case (pump laser on resonance, Stokes laser off resonance). From the initial state $|1\rangle$ (or $|2\rangle$), the populations are equally split on the two (a) and (b) paths in the sequence pump laser preceding the Stokes laser. At the end of the process, half of the population is continuously connected to the state $|2\rangle$ by the path (a) and half of the population to $|3\rangle$ by the path (b). If the system is initially prepared in the state $|2\rangle$, the sequence Stokes preceding pump pulse induces a coherent superposition of the states $|1\rangle$ and $|2\rangle$ [path (a)] without a relative dynamical phase.

$$\lambda^p_{\pm s} = \pm\frac{\hbar\Omega_p}{2}, \quad \lambda^p_{0s} = -\hbar\Delta_s \tag{7}$$

[where the first subscript index labels the eigenvalues (here $\pm$ or 0), the second subscript index (here s) is associated with the nonzero detuning and the superscript index (here p) corresponds to the nonzero field amplitude] are associated with the eigenvectors

$$|\pm\rangle^p_s = \frac{1}{\sqrt{2}}(|1\rangle \pm |2\rangle e^{i\epsilon_p\phi_p}), \quad |0\rangle^p_s = |3\rangle, \tag{8}$$

where $\epsilon_p=-1$ in the cases (a) and (b) and $\epsilon_p=1$ in the case (c). In the plane $\Omega_s=0$, the line continuously connected to the state $|3\rangle$ is thus associated with λ^p_{0s} (7), which crosses the line associated to the energy λ^p_{+s} at $\Omega_p=|2\Delta_s|$ (conical intersection).

In the plane $\Omega_p=0$, the eigenvalues are

$$\lambda^s_{\pm s} = \frac{\hbar}{2}(-\Delta_s \pm \sqrt{\Delta_s^2+\Omega_s^2}), \quad \lambda^s_{0s}=0, \tag{9}$$

with λ^s_{-s} and λ^s_{+s} associated to the states, respectively, $|2\rangle$ and $|3\rangle$ for $\Omega_s=0$.

The case 1-32 is depicted in Fig. 3 where the detunings are $\Delta_p/\delta=1$ and $\Delta_s/\delta=0$. The topology of the eigenenergy surfaces exhibits a conical intersection at

$$(\Omega_p,\Omega_s) = (0,2\Delta_p). \tag{10}$$

It coincides with the crossing of the two eigenvalues λ^s_{0p} and λ^s_{-p} in the plane $\Omega_p=0$ given by

$$\lambda^s_{\pm p} = \hbar(\Delta_p \pm \Omega_s/2), \quad \lambda^s_{0p}=0, \tag{11}$$

associated with the eigenvectors

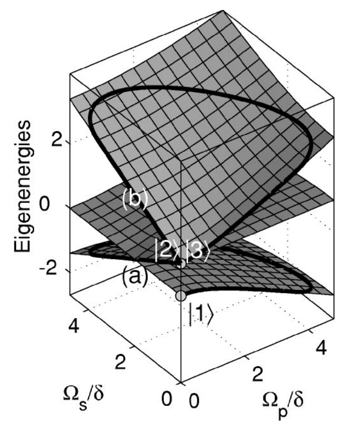

FIG. 3. Surfaces of eigenenergies as functions of the two Rabi frequencies Ω_p and Ω_s (in δ units) for the 1-32 case (pump laser off resonance, Stokes laser on resonance). Starting from the initial state $|2\rangle$ with the Stokes preceding the pump pulse, the population is equally split at the end of the process in the states $|1\rangle$ and $|2\rangle$. In the sequence Stokes following pump pulse, the paths (a) and (b) connect the states $|1\rangle$ and $|2\rangle$ to the coherent superposition of the states $|2\rangle$ and $|3\rangle$.

$$|\pm\rangle^s_p = \frac{e^{i\epsilon_p\phi_p}}{\sqrt{2}}(|2\rangle \pm e^{i\epsilon_s\phi_s}|3\rangle), \quad |0\rangle^s_p = |1\rangle, \tag{12}$$

where $\epsilon_s=1$ in the case (a) and $\epsilon_s=-1$ in the cases (b) and (c). In the plane $\Omega_s=0$, the eigenvalues of the Hamiltonian (1) are

$$\lambda^p_{\pm p} = \frac{\hbar}{2}(\Delta_p \pm \sqrt{\Delta_p^2+\Omega_p^2}), \quad \lambda^p_{0p} = \hbar\Delta_p; \tag{13}$$

λ^p_{+p}, λ^p_{0p} and λ^p_{-p} coincide, respectively, with the energies of the states $|2\rangle$, $|3\rangle$ and $|1\rangle$ for $\Omega_p=0$.

A. V-type system

1. Case 12-3

We describe the process in the V-type system, in which the population is initially in the state $|2\rangle$. We show below that the pulse sequence pump preceding Stokes laser leads to a coherent superposition of states $|2\rangle$ and $|3\rangle$. The pump field lifts the degeneracy of the eigenvalues $\lambda^p_{\pm s}$ (7) at zero field. The resonance of the $|1\rangle$ and $|2\rangle$ states is split such that the solution of the Schrödinger equation reads at early times ($t_i \to -\infty$) as

$$|\Psi(t_i)\rangle = |2\rangle = \frac{1}{\sqrt{2}}(|+\rangle^p_s + |-\rangle^p_s). \tag{14}$$

(Global phases are omitted throughout the paper, for simplicity.) The populations are equally divided on the paths (a) and (b) with energies λ^p_{-s} and λ^p_{+s}, respectively. The Stokes laser needs to be switched on *after* the crossing, i.e., when $\Omega_p > |2\Delta_s|$. The pump pulse falls to zero *before* the Stokes pulse induces a connection of the state $|-\rangle^p_s$ to the state $|2\rangle$ through the path (a) and the state $|+\rangle^p_s$ to the state $|3\rangle$ through the path (b) (see Fig. 2). Since the state $|1\rangle$ is decoupled of the others when the pump laser is off, no population can transit to this state by adiabatic passage. This leads, at the end of the process ($t_f \to +\infty$) to the coherent superposition,

$$|\Psi(t_f)\rangle = \frac{1}{\sqrt{2}}[e^{-i(\omega_s(t_f-t_i)+\phi_s)}|3\rangle - e^{i\varphi}e^{i\int_{t_i}^{t_f} dt(\lambda_{+s}(t)-\lambda_{-s}(t))}|2\rangle], \tag{15}$$

where $\lambda_{\pm s}$ are the eigenvalues of the effective Hamiltonian (1) with $\Delta_p=0$ (equal to $\lambda_{\pm s}^p$ and $\lambda_{\pm s}^s$ when $\Omega_s=0$ and $\Omega_p=0$, respectively). We like to stress that this superposition includes an optical phase relative to the Stokes laser $-i\omega_s(t_f-t_i)$, a dynamical phase (not robust with respect to the Stokes pulse amplitude) and an additional phase φ which needs to be evaluated by numerical integration of the Schrödinger equation: we find here $\varphi=\pi$. Below we show that the pulse sequence pump pulse following Stokes pulse leads to the coherent superposition of the states $|1\rangle$ and $|2\rangle$. Population follows the path (a) which leads to the *creation of the degeneracy* of the $|1\rangle$ and $|2\rangle$ states at zero field when the pump vanishes at the end of the process. The dynamics, controlled by the two pulses, follows adiabatically a *single eigenstate* (along the lower surface). This process generates the coherent superposition of these two states *without a relative dynamical phase*:

$$|\Psi(t_f)\rangle = \frac{1}{\sqrt{2}}[|1\rangle - e^{i\omega_p(t_f-t_i)}e^{i\phi_p}|2\rangle], \tag{16}$$

i.e., the relative phase between the components of the superposition does not depend on the pulse areas. This process can be seen as a half-SCRAP process where the Stokes laser acts as a Stark laser which shifts the conical intersection [23,24]. A comparison of the two superpositions of states (15) and (16) elaborated for $\Delta_p=0$ show an important difference: (i) the sequence pump preceding Stokes pulse induces two eigenstates independently populated during the process which leads to a superposition with a relative (not robust) dynamical phase; (ii) the sequence pump pulse following Stokes pulse populates a single eigenstate which leads to a superposition without relative dynamical phase. We anticipate that the superposition (16) is thus of particular interest with respect to applications requiring a controlled (i.e., nondynamical) phase as opposed to (15).

2. Case 1-32

In the 1-32 case where $\Delta_s=0$ (Fig. 3), the resonant Stokes pulse lifts the degeneracy if the pump laser follows the Stokes laser and generates two independent paths (a) and (b). By choosing the appropriate delay such that $\Omega_s > 2\Delta_p$ when the pump pulse is still off ($\Omega_p=0$), the path (a) passes through the crossing and allows one to connect $|2\rangle$ to $1/\sqrt{2}\,(|1\rangle-|2\rangle)$. This mechanism is well adapted for the construction of the superposition of the $|1\rangle$ and $|2\rangle$ states from the initial state $|2\rangle$. At the end of the process, we get

$$|\Psi(t_f)\rangle = \frac{1}{\sqrt{2}}[|1\rangle - e^{-i\int_{t_i}^{t_f} dt(\lambda_{+p}(t)-\lambda_{-p}(t))}e^{i(\phi_p+\omega_p(t_f-t_i))}|2\rangle]. \tag{17}$$

If the Stokes laser follows the pump laser, a single eigenstate is prepared, the dynamics along the upper surfaces [path (b)] follows this state adiabatically. The resulting state coincides, when the Stokes pulse vanishes, with the superposition of the states $|2\rangle$ and $|3\rangle$. Thus, in this pulse sequence, the coherent superposition of these two states is prepared without relative dynamical phase, i.e.,

$$|\Psi(t_f)\rangle = \frac{1}{\sqrt{2}}[|2\rangle + e^{-i\omega_s(t_f-t_i)}e^{-i\phi_s}|3\rangle]. \tag{18}$$

B. Ladder- and Λ-type systems

1. Case 12-3

For the processes in ladder- or Λ-type system, in which the population is initially in the state $|1\rangle$, the pulse sequence pump preceding Stokes leads to the coherent superposition of states $|2\rangle$ and $|3\rangle$ with a relative dynamical phase (see Fig. 2),

$$\text{ladder:}\quad |\Psi(t_f)\rangle = \frac{1}{\sqrt{2}}[e^{-i(\omega_s(t_f-t_i)+\phi_s)}|3\rangle - e^{i\int_{t_i}^{t_f} dt(\lambda_{+s}(t)-\lambda_{-s}(t))}|2\rangle], \tag{19}$$

$$\Lambda:\quad |\Psi(t_f)\rangle = \frac{1}{\sqrt{2}}[e^{i(\omega_s(t_f-t_i)+\phi_s)}|3\rangle - e^{i\int_{t_i}^{t_f} dt(\lambda_{+s}(t)-\lambda_{-s}(t))}|2\rangle]. \tag{20}$$

2. Case 1-32

The surfaces depicted in Fig. 3 show the possibility of preparing the coherent superposition of two excited states $|2\rangle$ and $|3\rangle$ from the initial state $|1\rangle$. In the sequence pump preceding Stokes pulse, the eigenenergy associated with the path (a) in the parameter space (Ω_p,Ω_s), starts from the energy associated with the state $|1\rangle$ and ends at the degeneracy of the states $|2\rangle$ and $|3\rangle$. In the adiabatic limit, the associated eigenstate transfers the population into the superposition of the states $|2\rangle$ and $|3\rangle$ in such a way that these two components have the same weights and no relative dynamical phase,

$$\text{ladder:}\quad |\Psi(t_f)\rangle = \frac{1}{\sqrt{2}}[|2\rangle - e^{-i\omega_s(t_f-t_i)}e^{-i\phi_s}|3\rangle], \tag{21}$$

$$\Lambda:\quad |\Psi(t_f)\rangle = \frac{1}{\sqrt{2}}[|2\rangle - e^{i\omega_s(t_f-t_i)}e^{i\phi_s}|3\rangle]. \tag{22}$$

C. Control of the weights of the components

As it has been studied in detail in [28], the distribution of the populations on two states which are initially quasi-

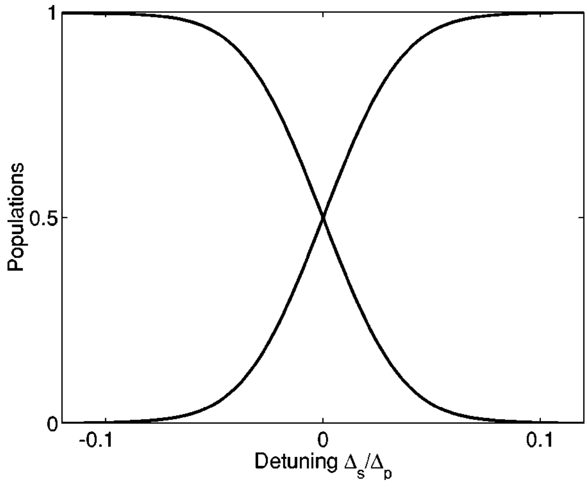

FIG. 4. Populations of the states $|2\rangle$ and $|3\rangle$ of a Λ- or a ladder-type system versus the one-photon detuning Δ_s in units of Δ_p after the interaction with two partially overlapping pulses. The pump pulse with Gaussian temporal shape and FWHM equal to $100\Delta_p$ is turned on first. A Stokes pulse with Gaussian temporal shape and FWHM equal to $100\Delta_p$ is delayed by $190\Delta_p$ with respect to the pump pulse. The amplitude of these two pulses are measured by the Rabi frequency: $\Omega_p=\Omega_s=4\Delta_p$.

degenerate, is adjustable by controlling the detuning Δ_s. For instance, in Fig. 4, we showed the populations of the states $|2\rangle$ and $|3\rangle$ after the interaction in the sequence pump pulse preceding Stokes pulse for various detunings Δ_s. This leads to the superposition (for a ladder-type configuration),

$$|\Psi(t_f)\rangle = [a|2\rangle - be^{-i\omega_s(t_f-t_i)}e^{-i\phi_s}|3\rangle], \quad |a|^2+|b|^2=1. \tag{23}$$

When this one-photon detuning is far from zero and negative ($\Delta_s T_s \ll 0$ with T_s the characteristic duration, e.g., the FWHM for a Gaussian pulse of the Stokes field), the population is completely transferred to the excited state $|2\rangle$. In the opposite case, when $\Delta_s T_s \gg 0$, we get a complete transfer into $|3\rangle$. In the intermediate regime ($|\Delta_s T_s| \ll 1$), we obtain the coherent superposition of states $|2\rangle$ and $|3\rangle$ with various weights. The weight of the two components depends on the value of the detuning Δ_s and in this sense, we get a technique to create a coherent superposition of two excited states with controllable weights. We like to remark that additional phases appear in the coefficients a and b of Eq. (23) depending on Δ_s and on the shape of the pulse (see [28]).

III. OPTIMIZATION OF ADIABATIC PASSAGE

The topology of the adiabatic passage gives a family of paths that connect an initial condition to a preselected superposition of states. It shows that the dynamics has to *globally* follow *adiabatically* a surface and also to *locally* jump *diabatically* through a crossing (or very close to it) from a surface to another. The success of population transfer by adiabatic passage depends thus not only on its topology, but also on the conditions that will allow negligible global nonadiabatic losses during the dynamics and local nondiabatic losses through the crossings (say a few percents). It is well-known that larger pulse areas will give smaller nonadiabatic losses in general. However in practice, it is of interest to determine for a given pulse shape, the parameters that will minimize the (nonadiabatic and nondiabatic) losses. This is how we define here the *optimization* of adiabatic passage.

The strategy to optimize is based on the analysis of Refs. [24,27]. There it is shown that in two-level systems driven by a chirped pulse, the nonadiabatic losses are minimized for given pulse shape and peak, when the dynamics follows a trajectory as a level line in the diagram of the eigenenergy difference in the parameter space. This means that a time representation of the eigenenergies should exhibit parallel lines. A particular level line is associated to specific losses, which can be in turn evaluated by the losses at early (or late) times: if the choice of a trajectory is made on a level line such that these losses at early times are negligible, this trajectory will be thus defined as an *optimal* one.

Here we will extend this strategy to a three-state system with the approximation to consider only the closest energy surfaces. The analysis is made on the example of the process described in Fig. 3, where we topologically generate the superposition of states $|2\rangle$ and $|3\rangle$ from the state $|1\rangle$ with the sequence pump preceding Stokes pulse and a single adiabatic state driving the population. The analysis can be extended to the other three state processes involving one single eigenstate.

This process described in Fig. 3 with the sequence pump preceding Stokes pulse is successful if the dynamics is globally adiabatic on the surface that connects $|1\rangle$ to the conical crossing (located at $\Omega_p=0$ and $\Omega_s=2\Delta_p$) and on the surface that connects this crossing to the degeneracy between the states $|2\rangle$ and $|3\rangle$, and locally diabatic to cross the crossing. We can easily determine a condition of adiabaticity at early times in the $\Omega_s=0$ plane where the upper and lower lines repel each other when Ω_p grows:

$$\Delta_p T_p \gg 1, \tag{24}$$

with T_p a characteristic duration (the FWHM of a Gaussian pulse) of the pump pulse. A condition of diabaticity near the crossing can be extracted from a local Landau-Zener analysis [28]. We suggest here alternatively to extend the analysis of Refs. [24,27].

Figure 5 shows the difference of the two lowest energy surfaces of Fig. 3 as a function of the two parameters Ω_p and Ω_s (in $\delta=\Delta_p$ units). These surfaces considered involve the state carrying the population and its closest neighbor. The contour plot exhibits level lines of constant energy and, according to the relations (10) a crossing (dark zone) corresponding to the conical intersection of the lines continuously connected to the states $|1\rangle$ and the degeneracy of $|2\rangle$ and $|3\rangle$. The dynamics can be characterized by a closed trajectory in the parameter space, starting and ending at $\Omega_p=\Omega_s=0$. We have designed one particular trajectory (white line), which combines minimum global nonadiabatic losses and no local nondiabatic loss. It indeed follows a level line in the plane $(\Omega_p>0,\Omega_s>0)$ and goes through the crossing ideally, i.e., for $\Omega_p=0$. This will lead to parallel lines in a time representation of eigenenergies apart around the crossing. The result

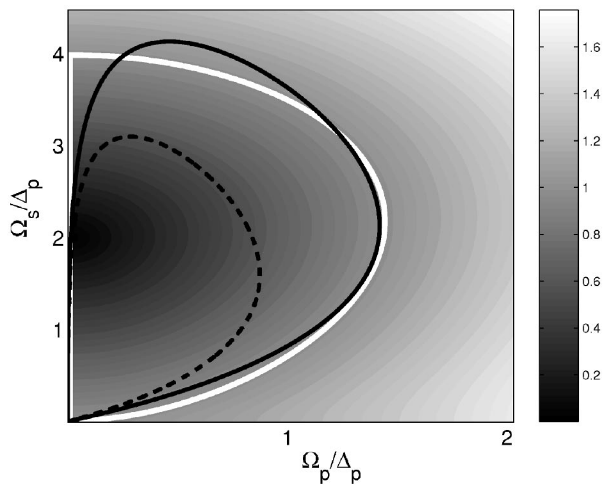

FIG. 5. Contour plot of the difference of the two lowest eigenvalues of the Hamiltonian (1) as a function of Ω_p and Ω_s (in $\delta = \Delta_p$ units). The white closed trajectory is an ideal trajectory generated by the field parameters that would allow optimal transfer of population from the state $|1\rangle$ to the coherent superposition of states $|2\rangle$ and $|3\rangle$ [see relation (21)] in the sequence pump preceding the Stokes pulse. The black trajectories are associated to the realization of this process in mercury atoms for pulses with a Gaussian temporal shape. The full black trajectory follows approximately the optimized level line represented by the white line. The dashed trajectory is used in Sec. V. The particular values of the field and atomic parameters are given in Sec. V.

of optimization can be thus formulated as follows in the approximation of closest neighbors: *Trajectories in this parameter space that minimize the losses lie on a level line in the plane* $(\Omega_p > 0, \Omega_s > 0)$ *and go through the crossing with* $\Omega_p = 0$.

This line requires that the Stokes field falls when the pump field is already zero.

If we consider the white line, an inspection of the contour of Fig. 5 gives approximate good optimizing peak values for the fields:

$$\Omega_p^{\max} \approx 1.3\Delta_p, \quad \Omega_s^{\max} \approx 4\Delta_p. \tag{25}$$

This condition (25) combined with (24) give good approximate values for the parameters $\Delta_p T_p$, $\Omega_s^{\max} T_p$ and $\Omega_p^{\max} T_p$. The other parameters have to be designed such that the trajectory characterizing the dynamics should be close to a level line (the white one if it is the one considered).

IV. THE TOPOLOGY OF STARK RAMAN ADIABATIC PASSAGE

In the preceding sections, we have seen that the topology does not allow us to connect the initial state to a superposition of $|1\rangle$ and $|3\rangle$ in Λ-, ladder- or V-type configuration by adiabatic passage. We recall that it is however possible if we allow overlapping fields with the control of the ratio of pump and Stokes pulse endings [19]. In what follows, we show that the construction of such a coherent superposition can be achieved using an additional Stark laser. We call this process Stark Raman adiabatic passage (STARAP). We propose mechanisms adapted to the configuration of the system respecting the experimental restrictions.

In addition to the pump and Stokes field, the three-state system interacts with an off resonant pulse that induces a Stark shift S_ℓ of the state $|\ell\rangle$. The effective Hamiltonian (1) reads as

$$H(t) = \frac{\hbar}{2}\begin{pmatrix} S_1(t) & \Omega_p(t) & 0 \\ \Omega_p(t) & 2\Delta_p + S_2(t) & \Omega_s(t) \\ 0 & \Omega_s(t) & 2(\Delta_p - \Delta_s) + S_3(t) \end{pmatrix}. \tag{26}$$

For a ladder or V system, the frequency of the Stark pulse is controlled in such a way that the shift of the upper state is predominant with respect to the shift undergone by the two lower states. In practice, this can be easily realized by approaching the frequency of the Stark laser around the Bohr frequency of a transition including the upper state and one of the numerous excited states. For a Λ system, we neglect the shift of the state $|3\rangle$. For the example of a magnetic system, this can be realized by controlling the polarization of the Stark field. The topology of eigenvalues surfaces is examined for various amplitudes of the pump (Ω_p) and Stokes (Ω_s) Rabi frequencies. We suppose that the Stark shifts are proportional to one of these two amplitudes.

A. Ladder system

For the case of a ladder-type configuration, we suppose that the system is prepared such that the population is in state $|1\rangle$. We assume that the Stark laser acts predominantly on the state $|3\rangle$ and the pump laser is chosen resonant. We thus neglect S_1 and S_2 in (26) and we take $\Delta_p = 0$, as described by Figs. 2 and 6 for the cases without and with an additional Stark laser. Two paths, on which the population is equally divided, are created by first switching on the pump laser. As shown in Fig. 2, they connect the state $|1\rangle$ to the states $|2\rangle$ and $|3\rangle$ in the absence of the Stark pulse. In order to use the paths (a) to connect the state $|1\rangle$ to itself and, thus, to achieve the coherent superposition of the states $|1\rangle$ and $|3\rangle$, we need an additional conical intersection. We make use of a negative Stark shift applied on the state $|3\rangle$ when the Stokes laser is off such that

$$\Lambda_0^p = \hbar(-\Delta_s + S_3/2) \tag{27}$$

crosses

$$\Lambda_-^p = -\frac{\hbar}{2}\Omega_p. \tag{28}$$

As a result, if the amplitude of the pump laser is strong enough to go through the conical intersection induced, we get the desired superposition as shown in Fig. 6. We like to remark that the sequence Stokes preceding pump pulse allows us to connect $|1\rangle$ to the superposition of $|1\rangle$ and $|2\rangle$ via the path (a) without a relative dynamical phase.

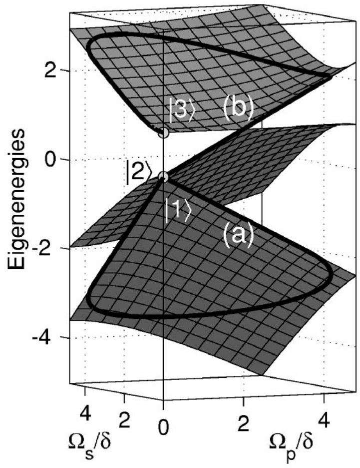

FIG. 7. Surfaces of eigenenergies as a function of the two Rabi frequencies Ω_p and Ω_s in δ units. A Stark laser, inducing a Stark shift with amplitude proportional to the amplitude of the Stokes laser ($S_1/2=-0.75\ \Omega_s$), is applied on the state $|1\rangle$ in order to decrease the associated eigenenergy Λ_0^s below the energy Λ_-^s (29). The two paths (a) and (b) are connected to the states $|1\rangle$ and $|3\rangle$. This process is well-adapted for a V-type configuration of states in which we get a coherent superposition of states $|1\rangle$ and $|3\rangle$ from the initial state $|2\rangle$.

B. V system

To induce the STARAP in systems with the V-type configuration, we have the choice to use a resonant Stokes laser or a resonant pump laser. We assume that the state $|1\rangle$ has the higher energy. It is realistic in an atom, to consider a predominant Stark shift of the state $|1\rangle$ and to neglect the shift of states $|2\rangle$ and $|3\rangle$. We thus use a resonant pump laser and

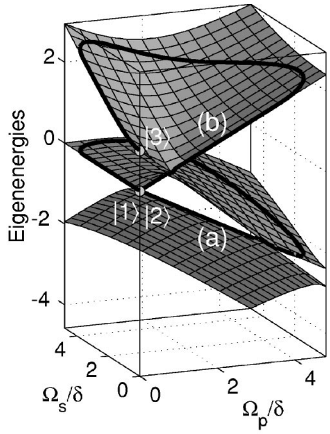

FIG. 6. Surfaces of eigenenergies as a function of the two Rabi frequencies Ω_p and Ω_s in δ units. A Stark shift with an amplitude proportional to the pump Rabi frequency (such that $S_3/2=-0.8$ -Ω_p), is applied on the state $|3\rangle$ in order to decrease the associated eigenenergy Λ_0^p (27) below the energy Λ_-^p (28). The two paths (a) and (b) are connected to the states $|1\rangle$ and $|3\rangle$, respectively. This process is well-adapted for a ladder-type configuration of states in which we get a coherent superposition of the states $|1\rangle$ and $|3\rangle$ in the sequence pump preceding Stokes pulse and of the states $|1\rangle$ and $|2\rangle$ in the sequence pump following Stokes pulse.

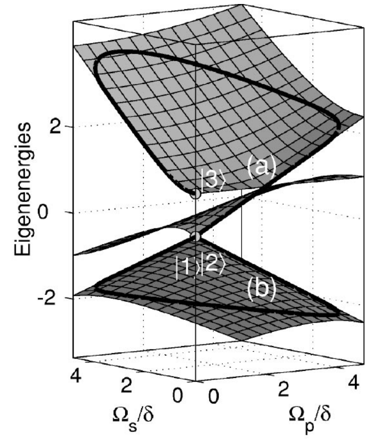

FIG. 8. Surfaces of eigenenergies as a function of the two Rabi frequencies Ω_p and Ω_s in δ units. A Stark laser, inducing a Stark shift with the amplitude proportional to the amplitude of the Stokes laser (such that $-S_1/2=S_2/2=0.4\ \Omega_s$), is applied on the transition $|1\rangle$-$|2\rangle$ by decreasing (increasing) the energy of the state $|1\rangle$ ($|2\rangle$). The two paths (a) and (b) connect the initial state $|1\rangle$ to the states $|3\rangle$ and $|1\rangle$, respectively. This process is well-adapted for a Λ-type configuration of submagnetic states in which we obtain the coherent superposition of the states $|1\rangle$ and $|3\rangle$. In the sequence Stokes preceding pump pulse, we create the coherent superposition of the states $|1\rangle$ and $|2\rangle$.

we choose the amplitude of the Stark shift such that

$$\Lambda_0^s = \frac{\hbar}{2}S_1 < \Lambda_-^s = -\frac{\hbar}{2}(\Delta_s + \sqrt{\Delta_s^2 + \Omega_s^2}), \qquad (29)$$

where Λ_0^s and Λ_-^s are, respectively, connected to $|1\rangle$ and $|2\rangle$ at zero field (see Fig. 7). The fields are considered in the pump-Stokes pulse sequence, and the amplitude of the pump laser is large enough such that the path (b) goes through the crossing between λ_{+s}^p and λ_{0s}^p (7). We get thus the superposition of the states $|1\rangle$ and $|3\rangle$ from the initial state $|2\rangle$, with a relative dynamical phase.

C. Λ system

For systems in a Λ-type configuration, the population is initially in the state $|1\rangle$ and as can be deduced from Fig. 8, the realization of STARAP is obtained by connecting this initial state to itself via the path (b). This connection is generated by exciting the transition $|1\rangle$-$|2\rangle$ via a nonresonant Stark pulse. We impose the frequency of the Stark laser to be smaller than the Bohr frequency associated with this transi-

TABLE I. Spectroscopic values of the considered transitions in mercury. λ is the wavelength of the transition, A_{12} is the Einstein coefficient for the spontaneous emission and the transition moment is labeled by μ.

Transition	λ (nm)	A_{12} (10^8 s^{-1})	μ (10^{-30} Cm)
$6^3P_1 \rightarrow 6^1S_0$	253, 728	0.08	2.15
$7^1S_0 \rightarrow 6^3P_1$	407, 898	0.0088	1.46

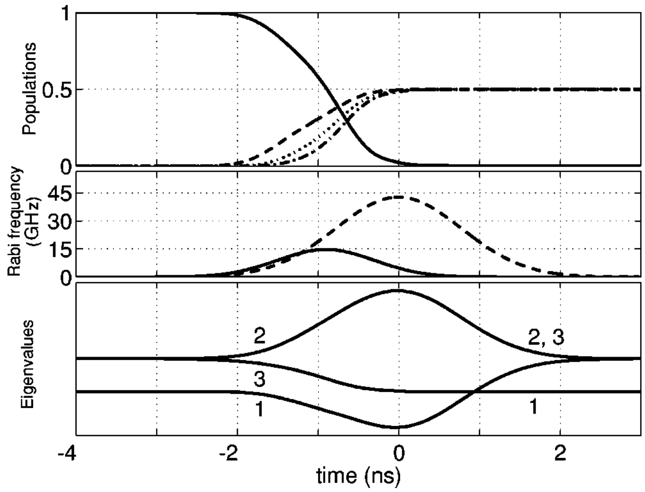

FIG. 9. Upper frame: populations as a function of time ($|1\rangle$, solid line; $|2\rangle$, dashed line; and $|3\rangle$, dash-dotted line). The real part of the product of the amplitudes associated with the occupancy probabilities of the states $|2\rangle$ and $|3\rangle$ is given by the dotted line. Middle frame: pump (full line) and Stokes (dashed line) Rabi frequencies. Lower frame: eigenvalues versus time. The numbers label the states that are connected when the fields are off. 2,3 means that the states $|2\rangle$ and $|3\rangle$ are degenerate at zero field.

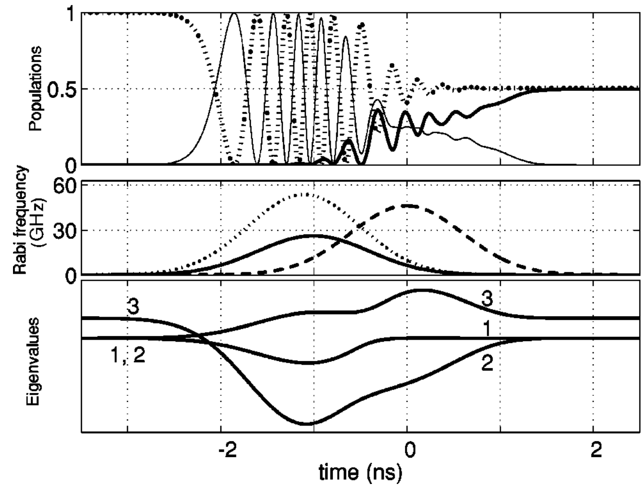

FIG. 10. Upper frame: populations as a function of time ($|1\rangle$, dotted line; $|2\rangle$, full thin line; and $|3\rangle$, in full large line). Middle frame: pump (full line) and Stokes (dashed line) Rabi frequencies. The Stark pulse (S_3) is depicted in dotted line. Lower frame: the eigenvalues versus time.

tion. We consider that the Stark effect undergone by the state $|3\rangle$ is negligibly weak with respect to the Stark effect undergone by the states $|1\rangle$ and $|2\rangle$.

In practice, such a realization could be obtained in a system of magnetic sublevels by appropriately choosing the polarization of the Stark laser. For a strong enough pump intensity, half of the population that follows the path (a) goes through the crossing between λ_{+s}^{p} and λ_{0s}^{p} (7) and the desired superposition of the states $|1\rangle$ and $|3\rangle$ is generated. In the Stokes-pump pulse sequence, we get the coherent superposition of the states $|1\rangle$ and $|2\rangle$ without a relative dynamical phase, as can be deduced from the path (b).

V. PROPOSED EXPERIMENTAL IMPLEMENTATION IN THE MERCURY ATOM

In this section, we demonstrate the reliability of some processes proposed in the preceding sections in the mercury atom. The three states of interest are the 6^1S_0, 6^3P_1 and 7^1S_0 labeled by $|1\rangle$, $|2\rangle$ and $|3\rangle$. The main features of the associated transitions are summarized in Table I.

We first apply the process described in Sec. II. We make use of a resonant Stokes pulse and a quasi-resonant pump pulse in the sequence pump preceding Stokes in order to create the coherent superposition of the states $|2\rangle$ and $|3\rangle$. This is associated with the topology of Fig. 3. The two pulses have Gaussian temporal shapes of FWHM 1 ns (pump) and 1.3 ns (Stokes). Their intensities are 0.07 MW/cm^2 and 1.26 MW/cm^2. The pulses are time delayed by 0.9 ns. These pulse parameters have been derived as follows: the frequency of the Stokes pulse is given by the Bohr frequency of the transition $|2\rangle$-$|3\rangle$, whereas the pump frequency is detuned of $\Delta_p T_p = 10.3$ such that the condition (24) is fulfilled in the nanosecond regime chosen here. Their intensities are chosen such that $\Omega_p^{\max}/\Delta_p = 1.4$ and $\Omega_s^{\max}/\Delta_p = 4.1$, to satisfy the condition (25). The delay as well as the duration of the Stokes pulse are adjusted such that the eigenvalue that drives the dynamics follows as close as possible the ideal white level line in the contour plot in Fig. 5. The resulting dynamics is characterized by the black full line in Fig. 5. We show in Fig. 9 the evolution of the three eigenvalues: one connecting the state $|3\rangle$ to the state $|1\rangle$ is approximately parallel for negative time (before the crossing) to the one connecting $|1\rangle$ to the $|2\rangle$ and $|3\rangle$ states, as expected from the optimization of the pulse parameters. At the end of the process, the populations of the states $|2\rangle$ and $|3\rangle$ are approximately 0.499 and 0.500, respectively. By changing the intensities of the pulses ($\Omega_p^{\max}/\Delta_p = 0.9$ and $\Omega_s^{\max}/\Delta_p = 3.1$) such that the dynamics (a black dashed trajectory in Fig. 5) does not follow precisely a level line the populations of the two excited states are approximately both 0.485 which is quite close to 0.5. This example illustrates the optimization of the transfer as well as the robustness of the process with respect to the amplitude of the fields.

We next apply the process described in Sec. IV A in order to create the coherent superposition of the states $|1\rangle$ and $|3\rangle$. This refers to the topology of Fig. 6. The pump is switched on before the Stokes pulse with a delay of 1 ns. The pulses are of Gaussian temporal shape with FWHM 1 ns. The intensities are 0.22 MW/cm^2 (pump) and 1.5 MW/cm^2 (Stokes). The Stark effect acts on the energy of the state $|3\rangle$, decreasing the energy by a maximum amplitude of 53.7 GHz. The Stark shift is generated by a pulse of Gaussian temporal shape with the same duration like the Stokes and the pump pulses and delayed by 1.1 ns with respect to the Stokes pulse. In Fig. 10, we show the spectrum of eigenvalues versus time. The state $|1\rangle$ is connected to the state $|3\rangle$, $|2\rangle$ to $|3\rangle$, and the state $|3\rangle$ that carries no population, is connected to the state $|2\rangle$.

VI. CONCLUSION

We have introduced and discussed alternative mechanisms for the construction of coherent superpositions in three-state systems by adiabatic passage with partially overlapping pulses. Two pulses, one resonant and one quasiresonant, are used and induce a degeneracy of the eigenstates at zero field. One particular pulse sequence (depending on the configuration and on the resonance considered) of pulses leads to population dynamics governed by two eigenstates. The other sequence leads to population dynamics governed by single eigenstates. In the first case, a lifting of the degeneracy is involved which splits the populations in two eigenstates with equal distribution in the case of exact resonance. In the second case, a creation of degeneracy occurs.

Furthermore, we gave a method to obtain a set of optimized pulse parameters from which the global nonadiabatic and the local nondiabatic losses are minimized. We have also shown that the coherent superposition of two states linked by a Raman type transition can be generated using an additional off-resonant Stark laser. A strong pump pulse shifts the degeneracy by creating two adiabatic states, on which the population is equally split.

The distribution of the populations is controllable, in all cases, by appropriately choosing the frequency of the resonant pulse which becomes near resonant. The stimulated adiabatic transfer and the Stark Raman adiabatic passage are robust with respect to moderate fluctuations in the intensity of the pulses and also against the variations in the pulse durations and in the delay between the two pulses. We proposed the implementation of these processes by realizing the coherent superposition of the 6^3P_1 and 7^1S_0 states of the mercury atom from the initial ground state 6^1S_0 by using two nanosecond pulses. Moreover the coherent superposition of the states $6\,^1S_0$ and $7\,^1S_0$ of the same atom using the additional interaction with a nanosecond Stark pulse should be possible.

ACKNOWLEDGMENTS

We acknowledge K. Bergmann, M. Fleischhauer, H. R. Jauslin, J. Klein, T. Rickes, B. W. Shore, and R. Unanyan for valuable discussions. N.S. is grateful for the kind hospitality at the Universität Kaiserslautern and acknowledges support through the Marie-Curie-Trainings site HPMT CT 2001-000294, established at the University of Kaiserslautern.

[1] M. Jain, Hui Xia, G. Y. Yin, A. J. Merriam, and S. E. Harris, Phys. Rev. Lett. **77**, 4326 (1996).

[2] A. J. Merriam, S. J. Sharpe, H. Xia, D. Manuszak, G. Y. Yin, and S. E. Harris, Opt. Lett. **42**, 625 (1999).

[3] M. D. Lukin, P. R. Hemmer, M. Loeffler, and M. Scully, Phys. Rev. Lett. **81**, 2675 (1998).

[4] P. Hemmer, D. Katz, J. Donaghue, M. Cronin-Colomb, M. Shahriar, and P. Kumar, Opt. Lett. **20**, 982 (1995).

[5] M. Jain, H. Xia, G. Y. Yin, A. J. Merriam, and S. E. Harris, Phys. Rev. Lett. **77**, 4326 (1996).

[6] K. Hakuta, M. Suzuki, M. Katsuragawa, and J. Z. Li, Phys. Rev. Lett. **79**, 209 (1997).

[7] A. Merriam, S. J. Sharpe, H. Xia, D. Manuszak, G. Y. Yin, and S. E. Harris, Opt. Lett. **24**, 625 (1999).

[8] A. V. Sokolov, D. R. Walker, D. D. Yavuz, G. Y. Yin, and S. E. Harris, Phys. Rev. Lett. **85**, 562 (2000).

[9] S. A. Myslivets A. K. Popov, T. Halfmann, J. P. Marangos, and T. F. George, Opt. Commun. **209**, 335 (2002).

[10] E. Korsunsky, T. Halfmann, J. P. Marangos, M. Fleischhauer, and K. Bergmann, Eur. Phys. J. D **23**, 167 (2003).

[11] T. Rickes, J. P. Marangos, and T. Halfmann, Opt. Commun. **227**, 133 (2003).

[12] P. Brumer and M. Shapiro, Annu. Rev. Phys. Chem. **43**, 257 (1992).

[13] C. P. Williams and S. H. Clearwater, *Explorations in Quantum Computing* (Springer-Verlag, Berlin, 1997).

[14] D. Bouwmeester, A. K. Ekert, and A. Zeilinger, *The Physics of Quantum Information: Quantum Cryptography, Quantum Teleportation, Quantum Computation* (Springer-Verlag, Berlin, 2000).

[15] P. Marte, P. Zoller, and J. L. Hall, Phys. Rev. A **44**, R4118 (1991).

[16] M. Weitz, B. C. Young, and S. Chu, Phys. Rev. A **50**, 2438 (1994).

[17] L. S. Goldner, C. Gerz, R. J. C. Spreeuw, S. L. Rolston, C. I. Westbrook, W. D. Phillips, P. Marte, and P. Zoller, Phys. Rev. Lett. **72**, 997 (1994).

[18] J. Lawall and M. Prentiss, Phys. Rev. Lett. **72**, 993 (1994).

[19] N. V. Vitanov, K.-A. Suominen, and B. W. Shore, J. Phys. B **32**, 4535 (1999).

[20] V. A. Sautenkov, C. Y. Ye, C. Y. Rostovtsev, G. R. Welch, and M. O. Scully, e-print quant-ph/0311076, http://xxx.lanl.gov

[21] R. Unanyan, M. Fleischhauer, B. W. Shore, and K. Bergmann, Opt. Commun. **155**, 144 (1998).

[22] R. Unanyan, B. W. Shore, and K. Bergmann, Phys. Rev. A **59**, 2910 (1999); F. Vewinger, M. Heinz, R. G.. Fernandez, N. V. Vitanov, and K. Bergmann, Phys. Rev. Lett. **91**, 213001 (2003).

[23] L. P. Yatsenko, N. V. Vitanov, B. W. Shore, T. Rickes, and K. Bergmann, Opt. Commun. **204**, 413 (2002).

[24] S. Guérin and H. R. Jauslin, Adv. Chem. Phys. **125**, 147 (2003).

[25] S. Guérin, L. P. Yatsenko, and H. R. Jauslin, Phys. Rev. A **63**, 031403(R) (2001).

[26] L. P. Yatsenko, S. Guérin, and H. R. Jauslin, Phys. Rev. A **65**, 043407 (2002).

[27] S. Guérin, S. Thomas, and H. R. Jauslin, Phys. Rev. A **65**, 023409 (2002).

[28] L. P. Yatsenko, S. Guérin, and H. R. Jauslin, Phys. Rev. A (to be published).